SANDIA REPORT
SAND2007-8012
Unlimited Release
Printed December 2007

Initial Case for Splitting Carbon Dioxide to Carbon Monoxide and Oxygen

James E. Miller

Sandia National Laboratories

Initial Case for Splitting Carbon Dioxide to Carbon Monoxide and Oxygen

James E. Miller
Sandia National Laboratories
P.O. Box 5800
Albuquerque, NM 87185-1349

Abstract

The United States presently imports almost ⅔ of the more than 20 million barrels of petroleum that it consumes daily. The largest fraction of this consumption, again about ⅔, is for transportation. Unfortunately, much of the non-domestic oil extraction, which we both directly and indirectly rely on, is from fields in unstable parts of the world. The national security and economic implications of our dependence upon foreign oil as well as the dangers of climate change resulting from green house gas emissions prompts a search for alternative sources of liquid fuels. Independence from problematic oil producers can be achieved to a great degree by applying decades-old synfuel technologies to convert non-conventional resources such as coal, oil-shale and tar-sands into liquid fuels. Unfortunately tapping into and converting these resources into liquid fuels only exacerbates green house gas emissions as they are carbon rich, but hydrogen deficient. Additionally, deploying these technologies requires large investments in time and capital.

The "hydrogen economy" is a newer alternative, but it poses significant infrastructure and technological challenges. However, if we adopt revolutionary thinking about energy and fuels, it may be possible to the meet the future fuel challenges while maintaining our traditional hydrocarbon fuel framework. We must recognize that hydrocarbon fuels are energy carriers, not energy sources. The energy stored in a hydrocarbon is released for utilization by oxidation to form CO_2 and H_2O. Furthermore, just as H_2O can be "re-energized" by applying energy to split water back into H_2 and O_2, hydrocarbons can be recycled by capturing CO_2 (and H_2O) and "re-energizing" them back into hydrocarbon form. *That is, there is a hydrocarbon analogy to the envisioned hydrogen economy that realizes the benefits of hydrogen while capitalizing on much of the existing liquid fuel infrastructure.* Of course, the only credible pathway for implementing this vision is through the application of persistent energy sources (e.g. solar or nuclear). In this document, the concept of applying high temperature thermochemical cycles to split CO_2 into CO and O_2 as a starting point for synthetic fuel production is introduced and potential advantages of this approach are discussed.

Table of Contents

List of Figures

5

List of Tables

1. Introduction

The United States presently imports almost ⅔ of the more than 20 million barrels of petroleum that it consumes daily. The largest fraction of this consumption, again about ⅔, is for transportation. Unfortunately, much of the non-domestic oil extraction, which we both directly and indirectly rely on, is from fields in unstable parts of the world. Thus, developing an independent, domestic source of transportation fuel is essential for the future security and economic well-being of the US. Additionally, the effect of unmitigated CO_2 releases on the global climate is a growing concern both here and abroad. Independence from problematic oil producers can be achieved to a great degree through the utilization of non-conventional hydrocarbon resources such as coal, oil-shale and tar-sands. However, tapping into and converting these resources into liquid fuels only exacerbates green house gas (GHG) emissions as they are carbon rich, but hydrogen deficient. Solving this conundrum within the traditional hydrocarbon fuel framework requires us to adopt revolutionary thinking about energy and fuels. We must recognize that hydrocarbon fuels are energy carriers, not energy sources. The energy stored in a hydrocarbon is released for utilization by oxidation to form CO_2 and H_2O. ***However, just as H_2O can be "re-energized" by applying energy to split water back into H_2 and O_2, hydrocarbons can be recycled by capturing CO_2 (and H_2O) and "re-energizing" them back into hydrocarbon form. That is, there is a hydrocarbon analogy to the envisioned hydrogen economy.*** Of course, the only credible pathway for implementing this vision is through the application of persistent energy sources (e.g. solar or nuclear).

The most general way to convert CO_2 and H_2O into a fuel is through the intermediate production of synthesis gas or "syngas". Syngas is roughly a 1:2 mixture of CO and H_2 whose exothermic conversion to fuel and other products is currently commercially practiced. Stated concisely, one key route to converting CO_2 and H_2O into fuel is the following "reenergizing" reaction:

$$2CO_2 + 4H_2O \rightarrow 2CO + 4H_2 + 3O_2$$
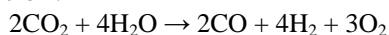
This reaction may of course be carried out either as written, or stepwise. For example, water splitting (WS) can be coupled with the reverse water gas shift reaction (RWGS) to produce syngas (Scheme 1).

Scheme 1	$6H_2O \rightarrow 6H_2 + 3O_2$
	$\underline{2CO_2 + 2H_2 \rightarrow 2CO + 2H_2O}$
	$2CO_2 + 4H_2O \rightarrow 2CO + 4H_2 + 3O_2$
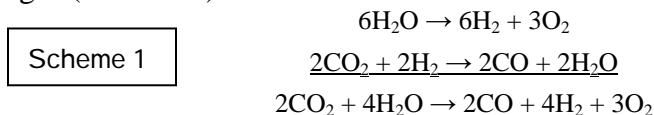
Recently, we proposed that it would be beneficial to split carbon dioxide and couple that reaction with the well known water gas shift reaction (WGS) to achieve the same result.

Scheme 2	$6CO_2 \rightarrow 6CO + 3O_2$
	$\underline{4CO + 4H_2O \rightarrow 4CO_2 + 4H_2}$
	$2CO_2 + 4H_2O \rightarrow 2CO + 4H_2 + 3O_2$
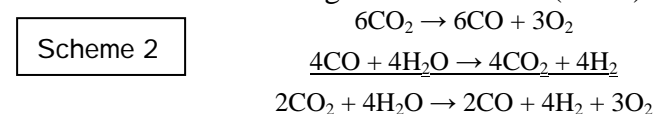
Herein, we begin to document and expand on the case for splitting carbon dioxide into CO and O_2 as an attractive alternative to water splitting.

2. Underlying Assumptions

In making the case for carbon dioxide splitting (CDS), we necessarily begin with several assumptions. First, we assume that the hydrogen economy makes sense. That is, most of

the assumptions that underlie the case for the hydrogen economy are necessarily incorporated here. These include assumptions regarding the desirability of increasing domestic sources of fuel and decreasing greenhouse emissions, as well as the assumption that the application of renewable/sustainable resources to fuel production, as opposed to production of electricity, is appropriate. Going further, for the purposes of this document, we assume that liquid fuels provide significant advantages over hydrogen such as compatibility with the current infrastructure. That is, the discussion herein is primarily limited to a comparison of water splitting and carbon dioxide splitting as the key steps in fuel production from CO_2 and water. The specific focus is on thermochemical processes as thermochemical water splitting is the most energy efficient approach to sustainable hydrogen production. The case for a CO_2 economy over a H_2 economy, or as an extension of the H_2 economy, remains to be made in detail elsewhere.

3. Thermodynamics of Water and Carbon Dioxide Splitting and the Water Gas Shift (WGS) Reaction

Carbon dioxide and water are extraordinarily stable molecules. As shown in Figure 1, thermodynamics does not favor their decomposition, even at 3000 °C. In addition to very high temperatures required, direct thermolysis is also made difficult in a practical sense by the inherent spatial coupling of the evolution of the different reaction products (H_2 and O_2, or CO and O_2). This coupling raises the possibility of recombination (possibly violent) and requires that difficult separations be performed.
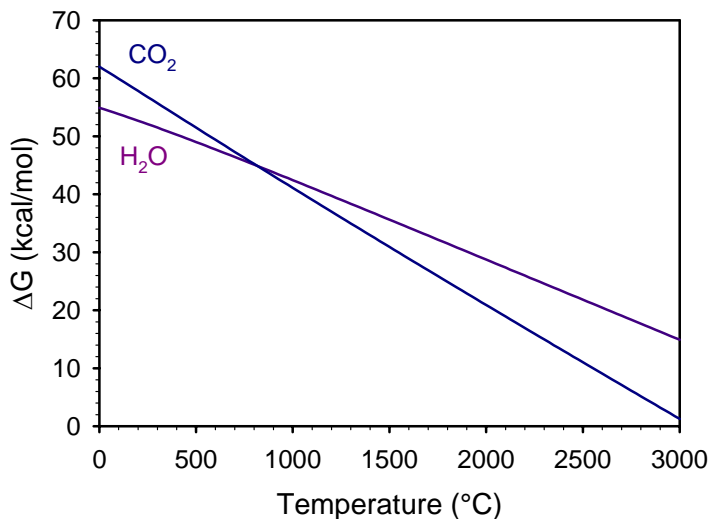
Figure 1. Free energy change for the reactions $H_2O \rightarrow H_2 + \frac{1}{2} O_2$ and $CO_2 \rightarrow CO + \frac{1}{2} O_2$ Calculations performed using HSC Chemistry for Windows software.

An interesting feature of the thermolysis reactions is that at temperatures above about 800 °C, CO_2 is less stable than H_2O, while at lower temperatures it is more stable. This fact has interesting consequences and implications that are the main topic of this paper.

Figure 2 compares the thermodynamics of water and CO_2 splitting assuming a CeO_2-based thermochemical cycle. Calculations indicate that CeO_2 spontaneously reduces (i.e. ΔG is negative) to Ce_2O_3 at temperatures above about 2350 °C. Note that while below

the reported melting point of CeO_2 (2600 °C) this temperature is above the melting point of the product Ce_2O_3 (2230 °C).[*] In practice, partial reduction of ceria to various sub-oxides is reported to be possible at lower temperatures.   In addition, the literature suggests that reduction temperatures can be lowered by alloying the ceria with other oxides, e.g. ZrO_2. Certainly this is the case for chemical reduction with hydrogen.   More interestingly, Figure 2 indicates that at any temperature below about 1500 °C, reduction of CO_2 to CO by Ce_2O_3 is thermodynamically favored, and furthermore, at temperatures greater than 800 °C, CO_2 reduction is more favored than water reduction.[†] This raises the possibility that CO_2 splitting can be accomplished with higher conversions (more negative ΔG) and higher reaction rates (at higher temperatures) than thermochemical water splitting.
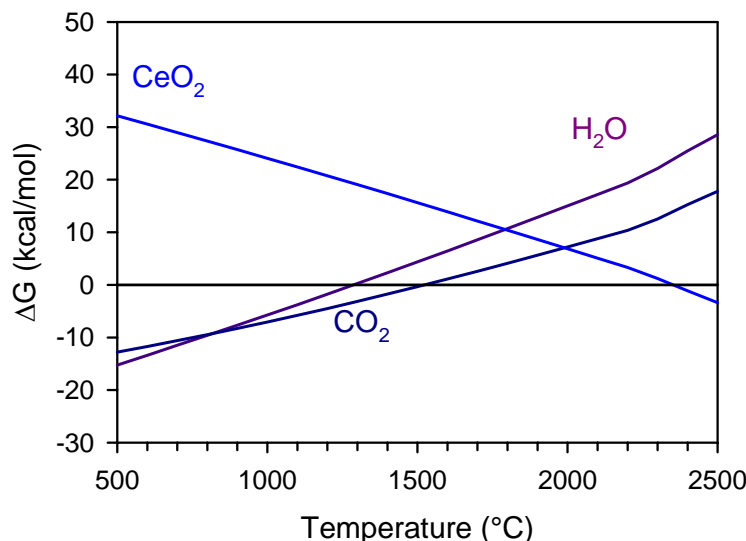
Figure 2. Free energy changes for ceria-based thermochemical water and CO_2 splitting.   Reactions are $CeO_2 \rightarrow \frac{1}{2} Ce_2O_3 + \frac{1}{4} O_2$; $Ce_2O_3 + H_2O \rightarrow 2 CeO_2 + H_2$; and $Ce_2O_3 + CO_2 \rightarrow 2 CeO_2 + CO$. Calculations performed using HSC Chemistry for Windows software.

Figure 3 illustrates a second key point resulting from the thermodynamics and in particular the crossover in the free energy that occurs at 800 °C. While CO_2 is less stable than water at temperatures > 800 °C, it is more stable than water at temperatures < 800 °C. Therefore, at temperatures < 800 °C, WGS favors the production of CO_2 and H_2. That is, H_2 can readily be produced through low-temperature WGS of CO with steam. Conversely, CO can not readily be produced by reacting H_2 with CO_2. Figure 3 shows

---

[*] The reduction of CeO_2 is calculated to occur at a lower temperature than that of Fe_3O_4 for which ΔG is negative for temperatures > 2830 °C. Furthermore, the melting points of the cerium oxides are higher than that of the Fe oxides (1538 °C for Fe_3O_4 and 1370 °C for FeO). Nonetheless we (and others) have been able to achieve good results for water splitting by thermally reducing Co-doped Fe_3O_4 mixed with ZrO_2 at 1400 °C.

[†] Currently we are reducing an excess of water at 1100 °C over a cobalt-doped ferrite. Calculations in HSC for the reaction of steam with FeO indicate that ΔG for the reaction is still positive at this temperature. However, at lower temperatures, the kinetics of the reaction are exceptionally slow. The calculations suggest that the combination of ceria and CO_2 (or even steam) will result in higher conversions with improved kinetics (more negative ΔG at higher temperatures).

that even very high temperatures do not drive the equilibrium completely towards CO and H_2O.
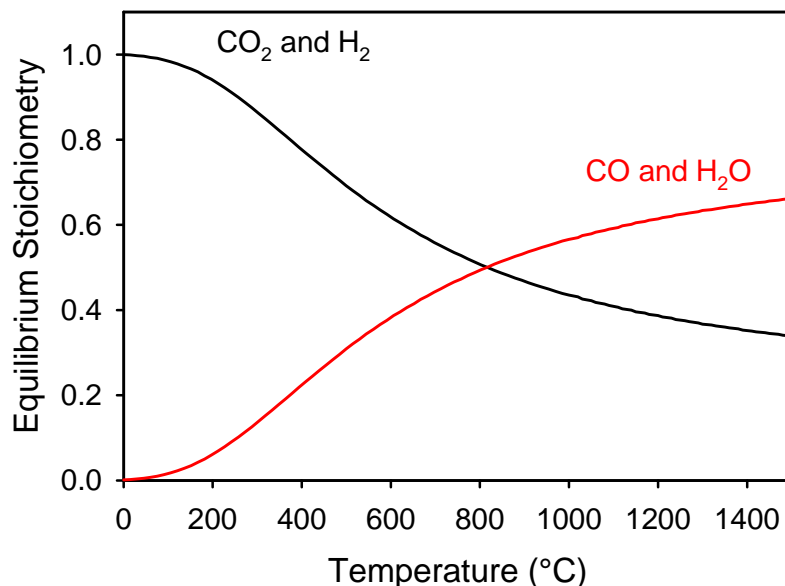
Figure 3. Thermodynamic equilibrium composition as a function of temperature for the WGS reaction $CO + H_2O(g) = CO_2 + H_2$. Note that equilibrium is practically independent of pressure.

The implications of this result are significant. First, it suggests that CO_2 should be considered as a working fluid for thermochemical hydrogen production cycles. In this case one must compare the cost of evaporating, heating, circulating, cooling and condensing excess steam to the cost of operating a WGS reactor and recovering CO_2 from H_2 for recycle. Operability issues for the two fluids should also be compared. For example, steam is known to promote the volatilization of metal oxides.

The second implication of this result pertains to the production of hydrocarbon fuels via a syngas intermediate. Figure 4A illustrates the WGS equilibrium for the stoichiometry 3:1 H_2:CO_2, the basic stoichiometry to produce a syngas product with 2:1 H_2:CO stoichiometry from H_2 and CO_2. The figure shows that the 2:1 stoichiometry is never realized for this gas mixture, even at a temperature of 900 °C. However, the temperature for 50% conversion of CO_2 to CO has shifted from 818 °C for the 1:1 mixture (Figure 3) to ca. 500 °C for the 3:1 mixture. Figure 5 illustrates the impact of using an even greater excess of H_2 in the feed relative to CO_2. For a 10:1 feed, 50% of the CO_2 is converted to CO at ca. 355 °C.

In contrast to the results for H_2 and CO_2, mixtures of CO and H_2O are quite capable of yielding 2:1 H_2:CO ratios. Figure 4B illustrates the WGS equilibrium for the stoichiometry 2:3 H_2O:CO, the basic ratio required to produce a 2:1 H_2:CO product. In this case, the equilibrium H_2:CO ratio ranges from 2 at 100 °C to 1.8 at 300 °C. That is, at any temperature < 300 °C, the equilibrium conversion of H_2O to H_2 is > 95%.
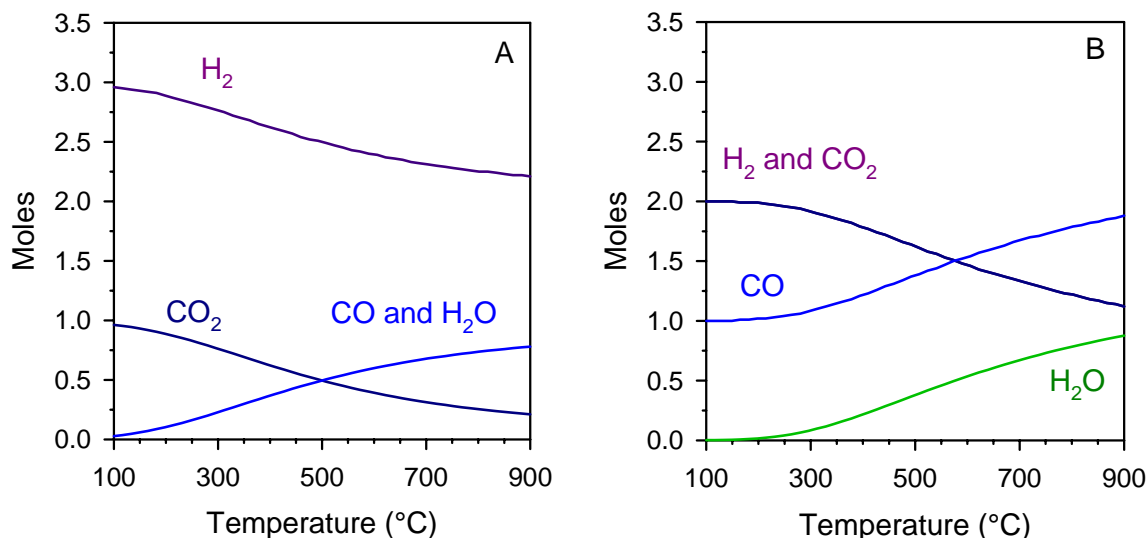
Figure 4. Thermodynamic equilibrium compositions as a function of temperature for the WGS reaction $CO + H_2O(g) = CO_2 + H_2$. A) Feed is 3:1 H_2:CO_2. B) Feed is 2:3 H_2O:CO.
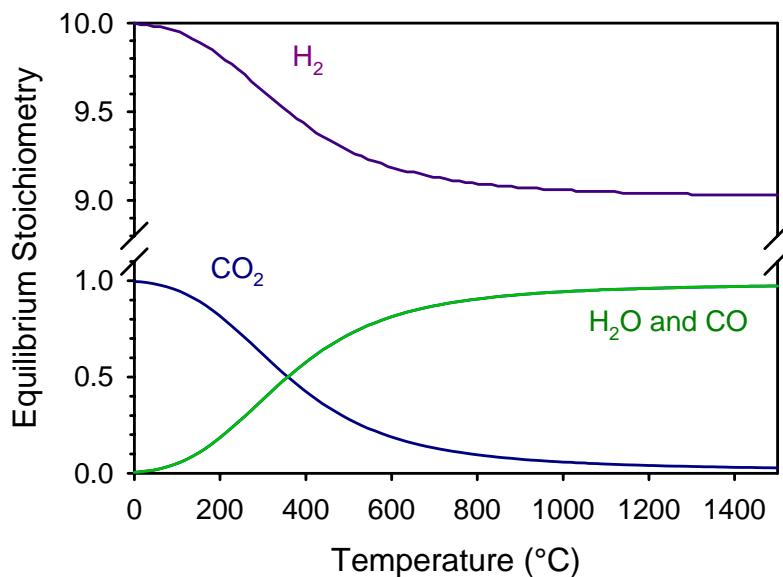
Figure 5. Thermodynamic equilibrium composition as a function of temperature for the WGS reaction $CO + H_2O(g) = CO_2 + H_2$. Feed is 10:1 H_2:CO_2.

4. Thermodynamics of Methanol Synthesis

The discussion above comparing WGS and RWGS chemistry is in some ways based on an oversimplification. In truth, there is not necessarily a requirement to perform a WGS or RWGS reaction to produce syngas in a separate step prior to producing a hydrocarbon product. That is, although WGS can be and is performed as a separate step, the WGS chemistry is also typically promoted by syngas-to-hydrocarbon catalysts. Additionally, if necessary, a catalyst bed of mixed functionalities is conceivable. Therefore, mixtures of

11

H_2 and CO_2 or mixtures of CO and steam can likely be more directly converted to a hydrocarbon product than perhaps implied by the earlier text.

Consider the example of methanol (CH_3OH). Methanol can be selectively produced from syngas in high yields and despite many shortcomings as a fuel, has recently been touted as an alternate to hydrogen [1]. The equilibrium yields from 2:1 H_2:CO mixtures[‡] are shown as a function of temperature and pressure in Figure 6. As indicated in the figure, operating conditions for the current technology are pressures of 50-100 bar and temperatures of ca. 250 °C. These conditions can theoretically result in per pass methanol yields in the range of 55-75%. Prior to World War II, less active catalysts were available and higher temperatures and pressures were required to achieve similar results.
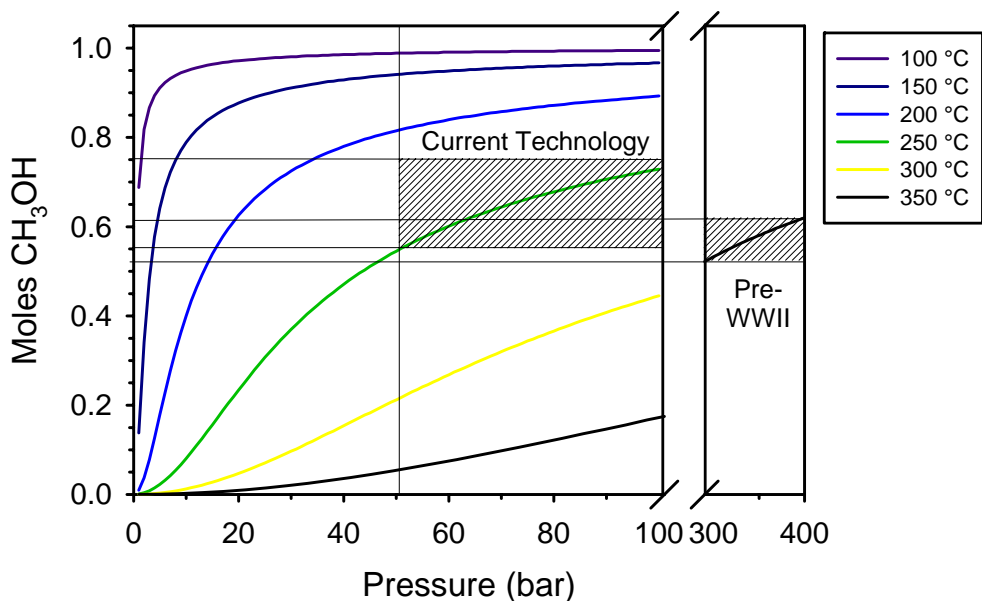
Figure 6. Thermodynamic equilibria for methanol synthesis from syngas $2H_2 + CO = CH_3OH$.

Figures 7 and 8 illustrate the equilibrium maximum methanol yields that could be expected from 3:1 mixtures of H_2 and CO_2 and 2:3 mixtures of H_2O and CO respectively. The 250 °C syngas curve and the "yield window" from Figure 6 is also shown in each figure for comparison. Figure 7 reveals that the possible equilibrium yields with the H_2-based approach fall far short of those achievable with syngas under similar conditions. Figure 8, however, indicates that potential per-pass yields with CO-based chemistry can exceed 50% at reasonable temperatures and pressures (i.e. 250 °C, 100 bar). Again, the reason for this difference can be traced to the basic thermodynamics of H_2O and CO_2. Both gas mixes H_2/CO_2 and H_2O/CO contain excess oxygen atoms relative to the stoichiometry of methanol. If methanol is produced, the excess oxygen must find its way into a coproduct. In the case of H_2/CO_2, the coproduct is water; in the case of H_2O/CO, the coproduct is CO_2. At the temperature of methanol synthesis, CO_2 is

---

[‡] "Real" feeds do not contain only CO and H_2. One way to account for the WGS reaction is to define a stoichiometric number as $(H_2-CO_2)/(CO+CO_2)$. The ideal stoichiometric number is 2 [2].

thermodynamically more stable than H_2O (Figure 1), hence the CO-based route is the more favorable alternate (non-syngas) route from an equilibrium standpoint.
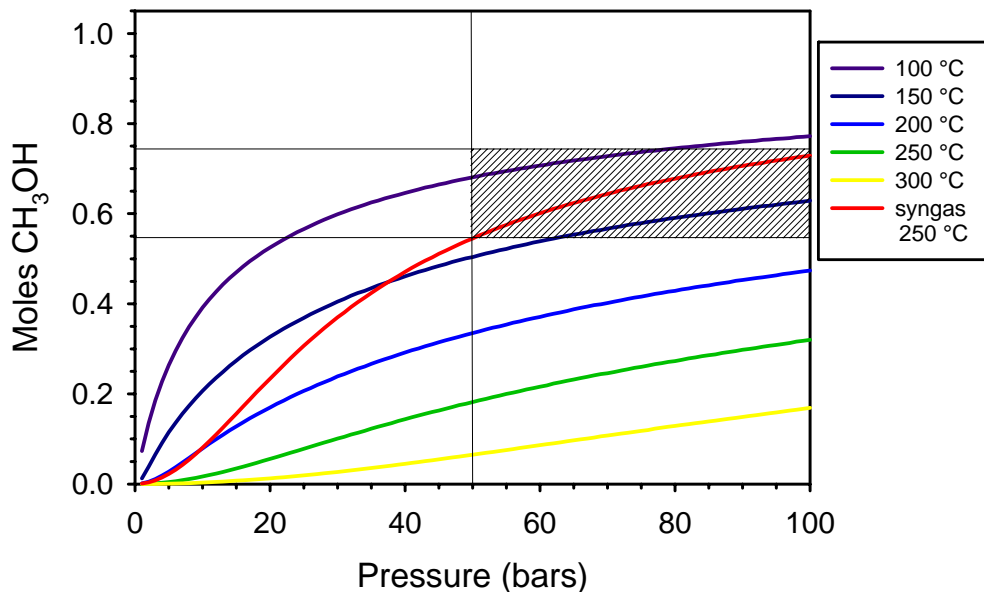
Figure 7. Thermodynamic equilibria for methanol synthesis from H_2 and CO_2. $3H_2 + CO_2 = CH_3OH + H_2O(g)$.
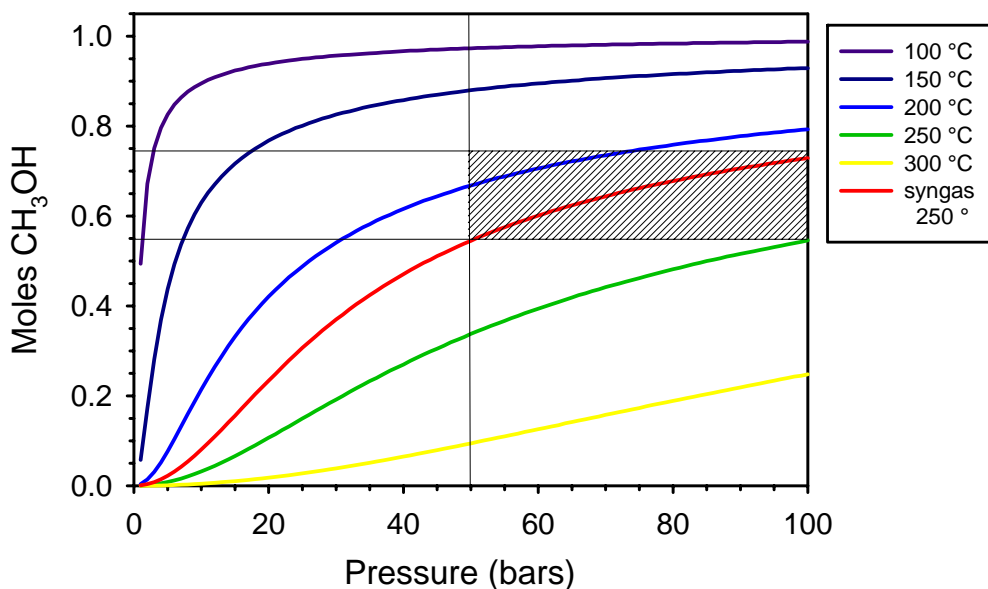
Figure 8. Thermodynamic equilibria for methanol synthesis from H_2O and CO. $2H_2O(g) + 3CO = CH_3OH + 2CO_2$.

In practice, per-pass conversions for methanol from syngas are significantly less than theoretical. Reported conversions range anywhere from only 15-25% [3] to as high as 40% [4] or 50% (with advanced catalysts) [5]. One limiting factor is the exotherm of the reaction which drives a temperature increase. The temperature increase suppresses the potential conversion, but conversion may also be intentionally limited to minimize the increase. There are several reactor design strategies for mitigating this effect, one of the

most advanced being the LPMeOH (liquid-phase methanol) reactor. In this case, the reaction is carried out in a large volume of inert liquid in which the catalyst is slurried. The large thermal mass of the inert prevents hot spots from developing and minimizes the overall temperature rise. A second strategy for improving per-pass conversions is the development of catalysts with improved activity as lower temperatures. Some progress in this regard has been reported, but evidently the materials rapidly deactivate [6].

5. Reaction Rates for Methanol Synthesis

Industrial syngas-to-methanol processes presently all rely on copper-based catalysts. The gas-phase ICI (now Synetix) process, which accounts for more than half of installed capacity, is based on a $Cu/ZnO/Al_2O_3$ catalyst [1]. Due to the maturity of the process the catalytic processes are well characterized if not fully understood and as such numerous kinetic models of methanol synthesis have been published. The steady-state model of Bussche and Froment [7] was formulated to be consistent with known reaction mechanisms occurring over $Cu/ZnO/Al_2O_3$ and was recently applied to perform initial cost estimates for converting H_2 and CO_2 to methanol [8].
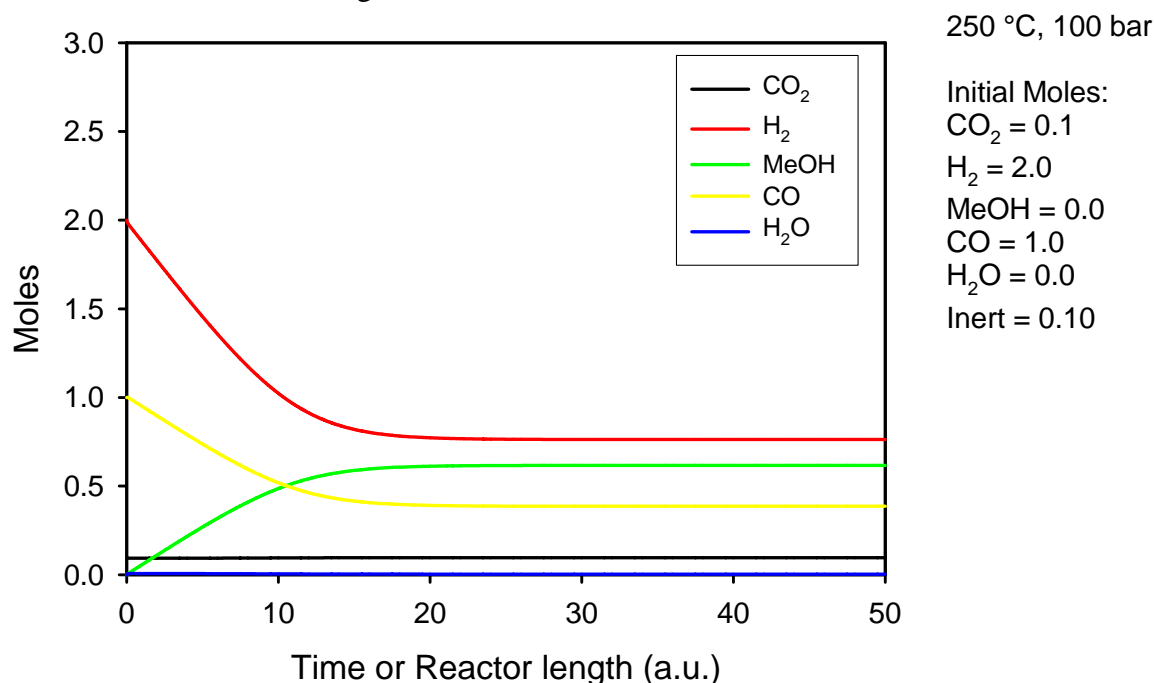
Figure 9. Calculated conversion of CO_2-containing synthesis gas to methanol over $Cu/ZnO/Al_2O_3$.

We have implemented a simplified version of the model in Sigmaplot (the reaction is treated as isothermal and isobaric) to provide an initial evaluation of the plausibility of methanol synthesis from alternate feeds by comparing results for syngas, H_2/CO_2 mixtures, and H_2O/CO mixtures. The model of a fixed-bed gas-phase plug flow reactor is based on reaction equilibria and rate equations for two different reactions of CO_2: the RWGS reaction and the direct hydrogenation of CO_2 to methanol. [§] The basic rate equations, material balances, and parameters used here are provided as Appendix A.

_____

[§] There is ample evidence suggesting that CO_2, rather than CO, is the direct precursor to methanol on the catalyst surface, e.g. through the formation of surface carbonates and formates.

The modeling results, normalized to a fixed catalyst loading, are presented in Figures 9-14. The results for a syngas feed containing a small fraction of CO_2 are presented in Figure 9. In this case, the reaction proceeds rapidly to the equilibrium composition. For Figure 10, the concentration of CO_2 in the feed is reduced by a factor of 10. In this case, the reaction is significantly more sluggish, reflecting the importance of CO_2 as a precursor to methanol. For Figure 11, the feed is again deficient in CO_2, but a small quantity of steam has been added to the feed. In this case, the evolution of methanol closely tracks that seen in Figure 9. This results from the initial rapid WGS reaction of H_2O and CO steam to form H_2 and the necessary CO_2.
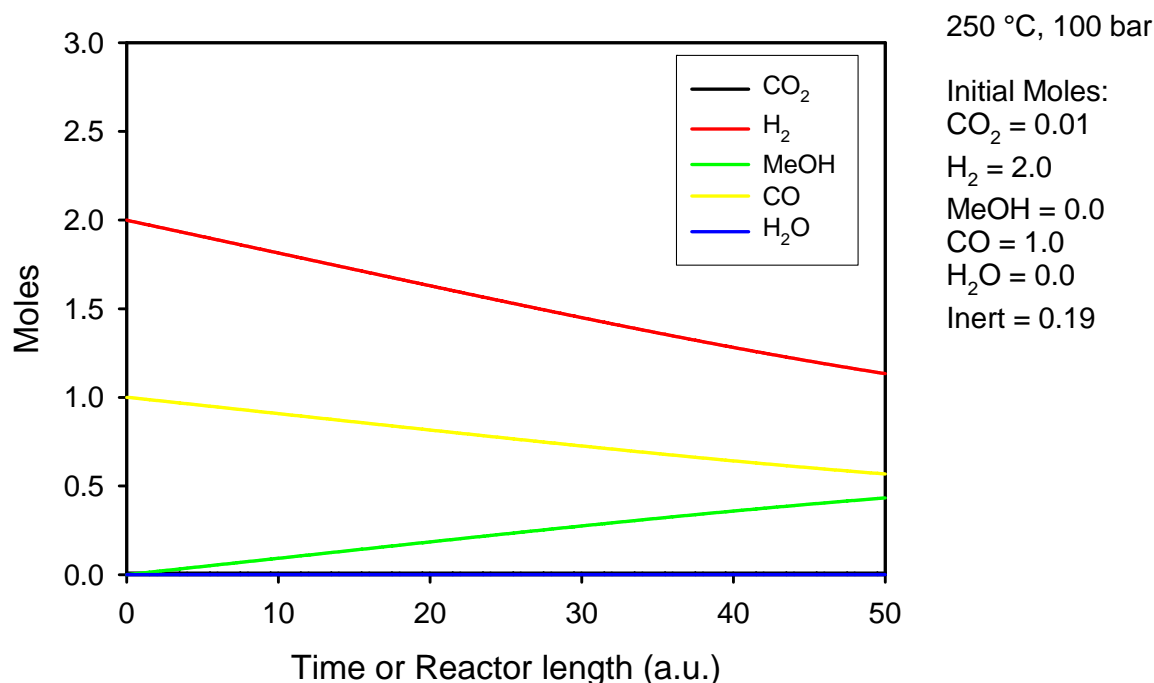
Figure 10. Calculated conversion of synthesis gas to methanol over $Cu/ZnO/Al_2O_3$. Syngas feed is dry and CO_2 deficient.

Results for a feed of 3:1 H_2:CO_2 are presented in Figure 12. In this case, the RWGS reaction results in an initial rapid conversion of H_2 and CO_2 to CO and H_2O. However, conversion to methanol is very slow despite the large amount of unconverted CO_2 remaining. Figure 13 shows that the kinetics are so sluggish that increasing the reactor length (or increasing the residence time) by a factor of four does not quite lead to an equilibrium mixture in the effluent. The reason underlying the sluggish kinetics is that water, a necessary co-product if CO_2 is to be the source of carbon, acts as an inhibitor on the catalyst. Note that the small amount of water was not an issue in Figure 11 because in that case it was rapidly consumed by WGS rather than produced by RWGS.
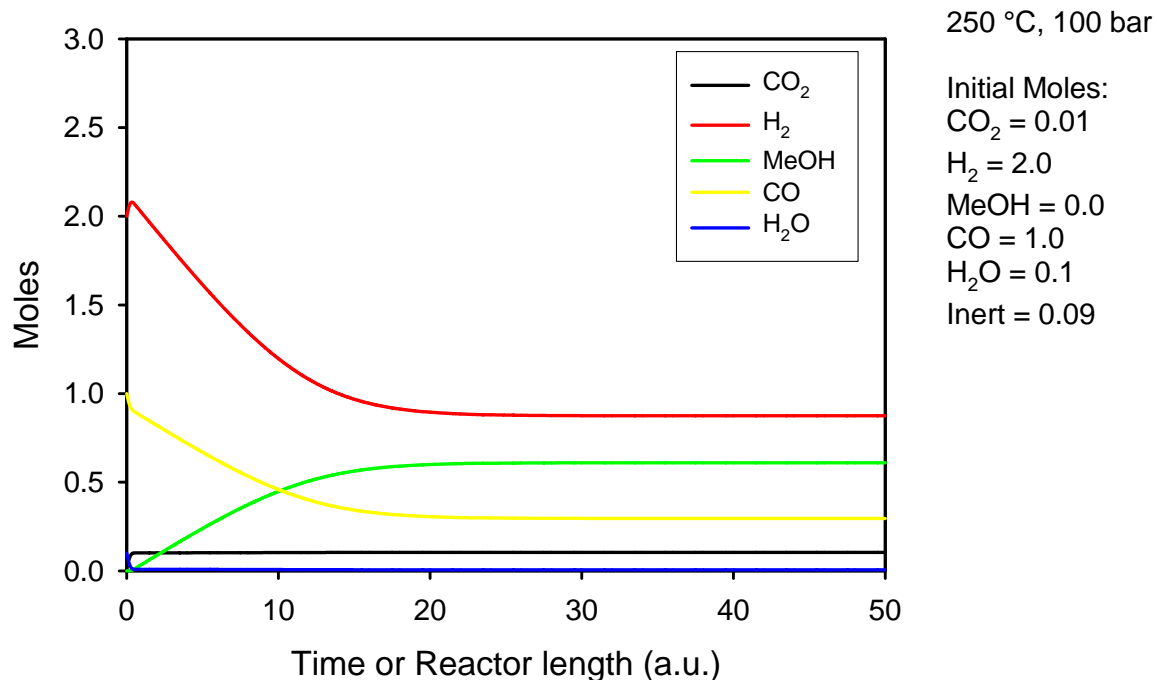
Figure 11. Calculated conversion of synthesis gas to methanol over Cu/ZnO/Al$_2$O$_3$. Syngas feed is CO$_2$ deficient, but moist.
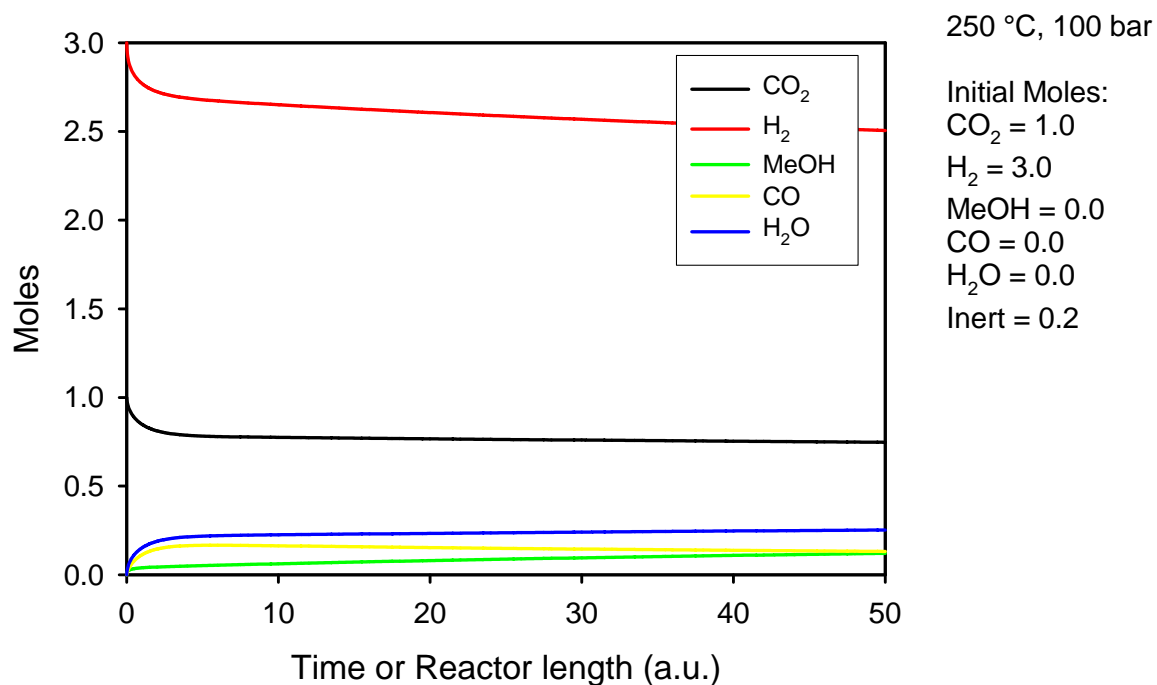
Figure 12. Calculated conversion of dry 3:1 H$_2$:CO$_2$ mixture to methanol over Cu/ZnO/Al$_2$O$_3$.
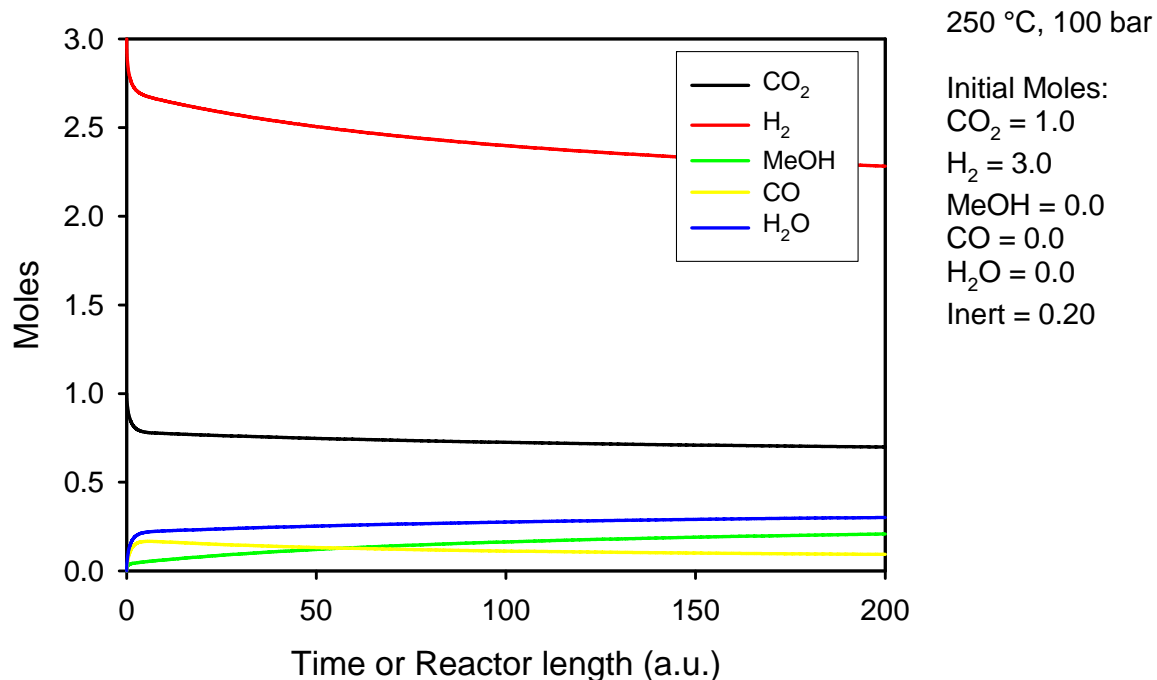
Figure 13. Calculated conversion of dry 3:1 H_2:CO_2 mixture to methanol over $Cu/ZnO/Al_2O_3$. Reactor (or residence time) has been lengthened by a factor of 4 to further illustrate sluggish kinetics.
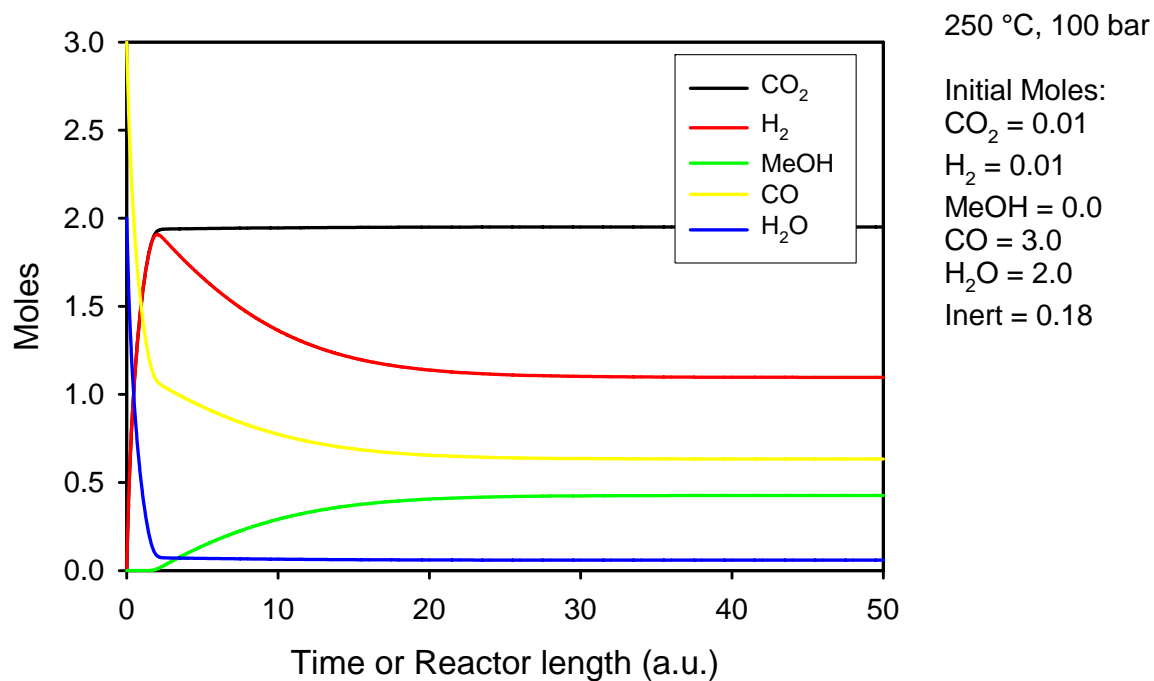
Figure 14. Calculated conversion of 3:2 CO:H_2O mixture to methanol over $Cu/ZnO/Al_2O_3$.

Figure 14 shows results for a 3:2 feed of CO and H_2O. In this case, there is again an initial rapid WGS reaction that results in the conversion of CO and H_2O into CO_2 and H_2. Although the consumption of water is not complete, it is evidently sufficient as the subsequent production of methanol proceeds apace. Unlike water, the presence of a large excess of CO_2 does not appear to be problematic, at least in this model. Hence, the

Bussche/Froment model indicates that from a reaction rate point of view, a mixture of CO and H_2O, while not as good as syngas, is again significantly better than a mixture of CO_2 and H_2 for methanol production. Clearly this conclusion needs validation.

Japanese researchers [9] and more recently others [10] have developed alternate catalysts for synthesizing methanol from CO_2 and H_2. The Japanese catalysts are Cu-Zn-based, but contain a variety of additives in addition to alumina including ZrO_2, Ga_2O_3, and SiO_2. Oddly, the list of properties the additives address, namely specific activity, active surface area (dispersion), thermal stability, and long term stability (sintering of support and active phases), does not include improved water tolerance. Clearly this was known to be an issue as experiments were done to show the negative effect of water on a $Cu/ZnO/ZrO_2$ catalyst. Similar experiments are not reported for the 4 and 5 component catalysts. Thus, it is not clear whether the advanced catalysts address the water issue. Per pass yields reported for the advanced catalyst are low (10%). We have repeated the modeling cases illustrated in Figures 9-14 using a model developed for one of the advanced Japanese formulations [11]. In general, the trends in the two models are similar, but the equilibrium conversions predicted by the model of Kubota el al. are a little higher. The notable exception is that the Japanese model does not indicate significant inhibition by water. It is not clear whether this is actually a representative result for the multicomponent catalyst or the result of applying the model beyond its applicable range The full set of results and further discussion are presented in Appendix B.

6. Thermodynamics of Dimethyl Ether (DME) Synthesis

Dimethyl ether (DME) has attracted interest as a clean-burning substitute for diesel. Similar to LPG, DME must be slightly pressurized for storage (saturated vapor pressure is 6.1 atm), but it has a higher cetane number (55-60) than LPG (5-10), methanol (5), or diesel fuel (40-55). The energy density is higher on a mass and volumetric (as liquid) basis than methanol [12].
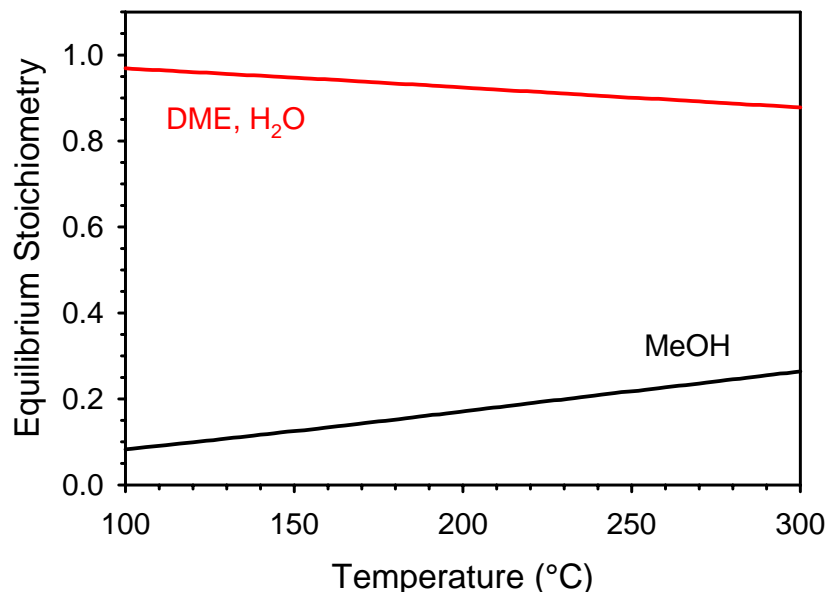
Figure 15. Thermodynamic equilibria as a function of temperature for methanol dehydration to DME ($2CH_3OH \leftrightarrow CH_3OCH_3 + H_2O$). Pressure has little effect on the equilibrium.

The traditional route to DME is the dehydration of methanol over an acid catalyst.

$$2CH_3OH \leftrightarrow CH_3OCH_3 + H_2O$$

However, if acidic functionality is included along with a methanol synthesis/WGS catalyst, the complete synthesis can be performed in a single reactor starting from syngas. This process intensification is interesting not only because the number of reactors is reduced, but also because the favorable thermodynamics (equilibria) of the dehydration reaction (Figure 15) can be used to drive to the methanol synthesis reaction, thereby increasing reactor productivity.

Another interesting twist to DME production is that there are two possible reactions:

1) $2CO + 4H_2 \leftrightarrow CH_3OCH_3 + H_2O$

2) $3CO + 3H_2 \leftrightarrow CH_3OCH_3 + CO_2$
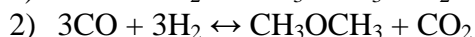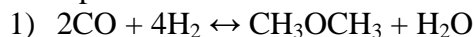
The equilibrium conversions for these two reactions are presented in Figures 16 and 17.

There are at least three important observations that can be made from a comparison of Figures 16 and 17. First, the equilibrium yields for either feed mixture, particularly the higher temperature yields, generally exceed those for methanol. Second, for a given temperature, the yields are higher for the 1:1 $CO:H_2$ mixtures than for the 1:2 mixtures. As in earlier discussions, this can be attributed to the greater thermodynamic stability of CO_2 as compared to H_2O at the temperatures of interest. That is, the oxidation of CO is more favorable than the oxidation of H_2 at these temperatures (Figure 1). Finally, the results have less pressure dependence than is observed for methanol synthesis.
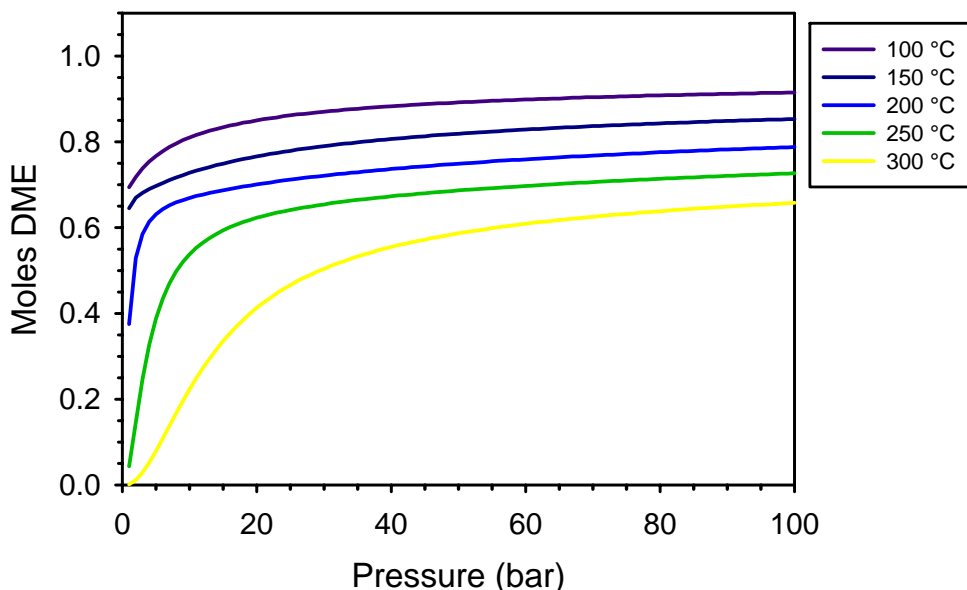
Figure 16. Thermodynamic equilibria as a function of temperature and pressure for DME synthesis from syngas with water as a co-product $(2CO + 4H_2 \leftrightarrow CH_3OCH_3 + H_2O)$.
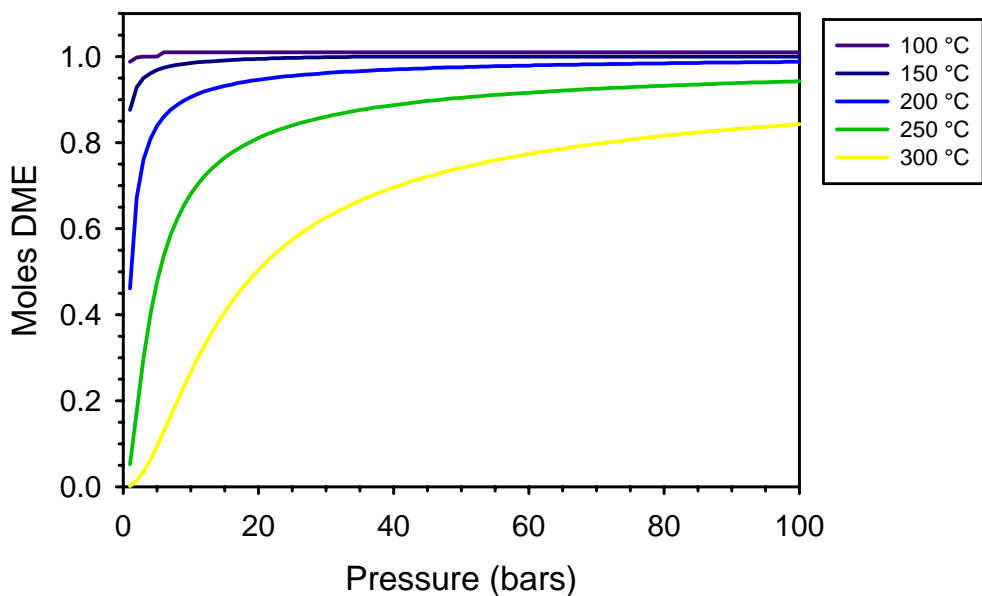
Figure 17. Thermodynamic equilibria as a function of temperature and pressure for DME synthesis from syngas with carbon dioxide as a co-product ($3CO + 3H_2 \leftrightarrow CH_3OCH_3 + CO_2$)

The results for a 3:1 Feed of H_2 and CO_2 are presented in Figure 18. In this case, the gains achievable over methanol synthesis are marginal, being roughly 5% net increase for a given temperature at 100 bars. The curves are somewhat flatter though and the gains are more significant at lower pressures. The results for a 2:1 $CO:H_2O$ feed are shown in Figure 19. In this case the yields are not quite as good as those for the CO_2-yielding syngas route, but they greatly exceed those possible with CO_2 and H_2 mixtures, and also exceed those from the water-yielding syngas route. The advantage over the syngas route increases at lower temperatures.
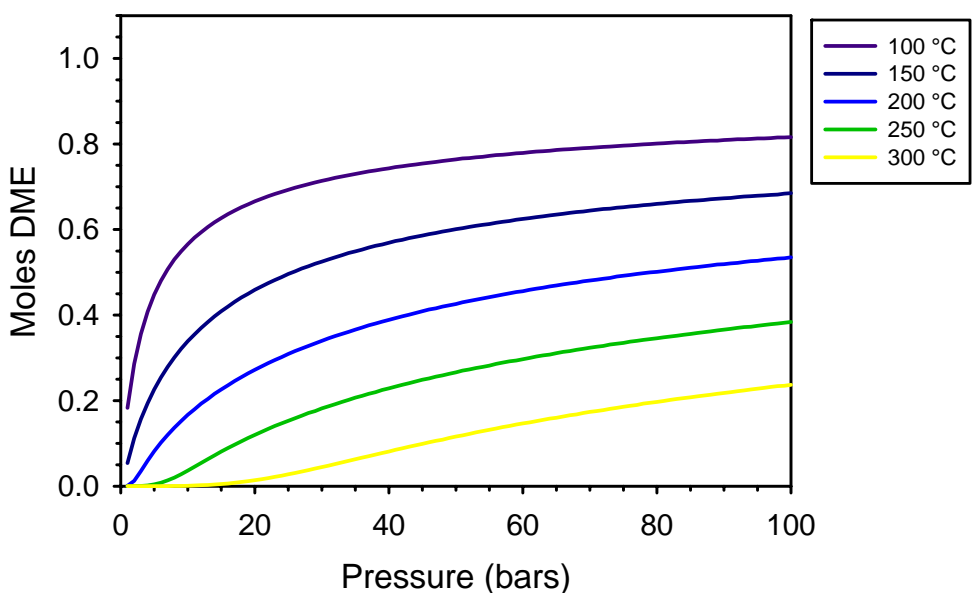
Figure 18. Thermodynamic equilibria as a function of temperature and pressure for DME synthesis from a 3:1 mixture of H_2 and CO_2 ($2CO_2 + 6H_2 \leftrightarrow CH_3OCH_3 + 3H_2O$).

There is a second potential advantage of the CO and H_2O route over the water-yielding syngas route and it again stems from the presence of water. In some cases the acid functionality of some materials can be rendered inactive by excess water [13]. Thus, in this case, the produced water is a potential issue for both the Cu-based methanol synthesis catalyst and the acidic dehydration catalyst. In the case of the CO/H_2O feed, the WGS reaction consumes water, potentially mitigating this problem. Of course, the CO_2-yielding syngas route likely negates this potential advantage. Also, the complete absence of water can in some cases also lead to catalyst deactivation through coking [13].
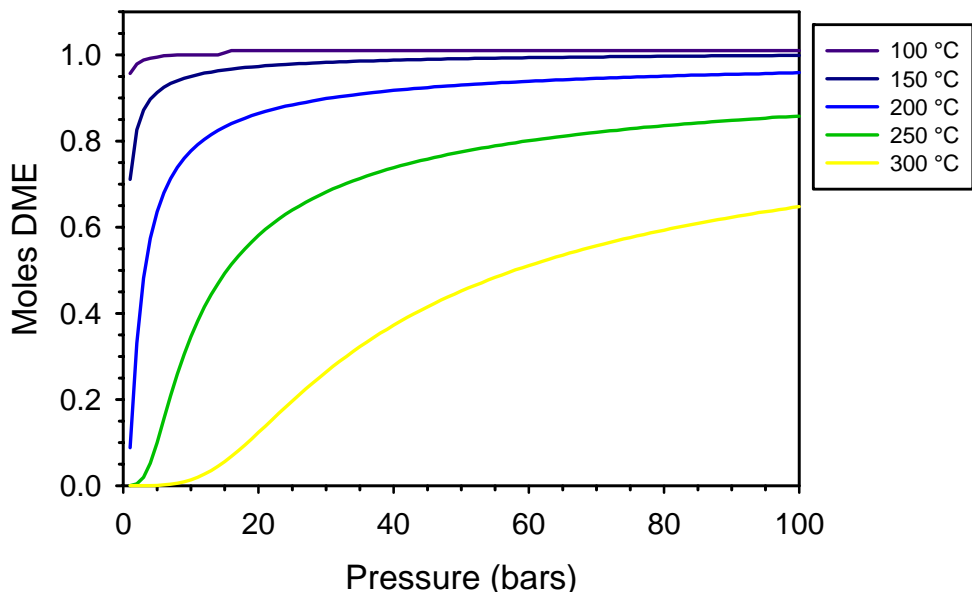
Figure 19. Thermodynamic equilibria as a function of temperature and pressure for DME synthesis from a 2:1 mixture of CO and H_2O ($6CO + 3H_2O \leftrightarrow CH_3OCH_3 + 4CO_2$).

7. Additional Thermodynamic Considerations

One of the practical difficulties of large-scale methanol synthesis is that the reaction is exothermic. Successfully managing the heat is a key to achieving high yields as the equilibrium becomes more unfavorable as temperature increases. There are several different approaches to this including the use of multiple reactors with cooling between sections, intermittent gas injection along the length of the reactor, and a unique annular design with external cooling and internal heat exchange that also preheats the reactor feed [5]. Carrying out the reaction using a slurry catalyst in an inert liquid phase acting as a thermal sink and heat transfer fluid as in the LPMeOH or LPDME process is one option that seems very promising [14]. The large thermal mass and intimate contact between the inert liquid phase and the reacting gaseous phase does much to minimize the temperature rise and increase yields.

The basic thermodynamics of the different reactions discussed herein are compared in Table 1. It is clear from the table that thermal management will be an even more important consideration for the most attractive alternatives to methanol from syngas discussed above. For example, the heat released for methanol synthesis from CO and

H_2O is almost double that for methanol from syngas. The situation for syngas to DME and CO_2 is worse, with higher potential yields and an exotherm that is more than 2.5 times greater than that for methanol synthesis. Worse yet is DME synthesis from CO and H_2O for which the exotherm is up to 4 times greater than that for methanol from syngas. Clearly if the advanced options discussed herein are to be successfully implemented, clever reactor designs to manage the heat evolution will be crucial.

Table 1. Thermodynamics of reactions relevant to methanol and DME synthesis.

Reaction	25 °C	100 °C	200 °C	300 °C	
1	-9.848	-9.747	-9.58	-9.374	ΔH (kcal)
WGS	-10.103	-9.797	-9.403	-9.008	ΔS (cal/K)
	-6.836	-6.091	-5.131	-4.211	ΔG (kcal)
2	-21.62	-22.339	-23.134	-23.76	ΔH (kcal)
Syngas to	-52.379	-54.535	-56.134	-57.636	ΔS (cal/K)
MeOH	-6.003	-1.989	3.567	9.274	ΔG (kcal)
3	-11.788	-12.591	-13.553	-14.386	ΔH (kcal)
CO_2 to MeOH	-42.33	-44.738	-47.028	-48.628	ΔS (cal/K)
& H_2O	0.833	4.102	8.698	13.485	ΔG (kcal)
4	-41.057	-41.833	-42.295	-42.507	ΔH (kcal)
CO to MeOH	-72.477	-74.130	-75.238	-75.652	ΔS (cal/K)
& CO_2	-19.676	-14.172	-6.696	0.853	ΔG (kcal)
5	-5.706	-5.516	-5.310	-5.158	ΔH (kcal)
MeOH to	-5.580	-5.009	-4.517	-4.224	ΔS (cal/K)
DME & H_2O	-4.043	-3.647	-3.173	-2.737	ΔG (kcal)
6	-48.947	-50.194	-51.578	-52.677	ΔH (kcal)
Syngas to	-110.337	-114.079	-117.379	-119.496	ΔS (cal/K)
DME & H_2O	-16.050	-7.625	3.960	15.812	ΔG (kcal)
7	-58.779	-59.941	-61.158	-62.051	ΔH (kcal)
Syngas to	-120.386	-123.876	-126.782	-28.503	ΔS (cal/K)
DME & CO_2	-22.886	-13.717	-1.171	11.601	ΔG (kcal)
8	-29.282	-30.699	-32.417	-33.93	ΔH (kcal)
CO_2 to DME	-90.240	-94.484	-98.572	-101.48	ΔS (cal/K)
& H_2O	-2.377	4.558	14.222	24.233	ΔG (kcal)
9	-88.276	-89.183	-89.899	-90.172	ΔH (kcal)
CO to DME &	-150.533	-153.268	-154.992	-155.527	ΔS (cal/K)
CO_2	-43.394	-31.991	-16.565	-1.031	ΔG (kcal)

1) $CO + H_2O = CO_2 + H_2$
2) $CO + 2H_2 = CH_3OH$ (methanol synthesis)
3) $CO_2 + 3H_2 = CH_3OH + H_2O$
4) $3CO + 2H_2O = CH_3OH + 2CO_2$
5) $2CH_3OH = CH_3OCH_3 + H_2O$ (methanol dehydration)
6) $2CO + 4H_2 = CH_3OCH_3 + H_2O$ (dimethyl ether synthesis)
7) $3CO + 3H_2 = CH_3OCH_3 + CO_2$
8) $2CO_2 + 6H_2 = CH_3OCH_3 + 3H_2O$
9) $6CO + 3H_2O = CH_3OCH_3 + 4CO_2$

8. Conclusions

Thermodynamics shows that at temperatures in excess of 850 °C, carbon dioxide splitting is favored over water splitting. Additional advantages such as improved operability may also be realized, but further study and validation of the potential is required. At low temperatures, CO is readily converted to H_2 via the WGS reaction. This suggests that CDS should be considered as a route to hydrogen. Going further, if the goal is the utilization or recycle of CO_2, then there are potential further advantages to CDS over WS. Specifically, the thermodynamics of methanol and DME synthesis and possibly the kinetics of methanol synthesis are much more favorable for mixtures of CO and H_2O than for CO_2 and H_2. That is, given the choice between "re-energizing" CO_2 and H_2O (to CO and H_2 respectively), thermodynamic equilibria and kinetic models both strongly suggest that CDS is the better option. This is not the final word, however. Additional process considerations such as heat management (reactor design), the difficulty and energy expenditure of the separations required, the amount of gas being pressurized, recovered, and recycled, capital costs, and the amount of technology development (e.g. improvements in catalysts) required must be considered in detail and weighed for each option before a true "best-choice" is identified. These and other considerations are under investigation and will be discussed in future publications.

9. References

1. G.A. Olah, A. Goeppert, and G.K.S. Prakash in <u>Beyond Oil and Gas: The Methanol Economy</u> Wiley-VCH, New York (2006).
2. J.-P. Lange "Methanol Synthesis: A Short review of Technology Improvements" Catal. Today **64**, 3 (2001).
3. X.-M. Liu, G.Q. Lu, Z.-F. Yan, J. Beltramini "Recent Advances in Catalysts for Methanol Synthesis via Hydrogenation of CO and CO_2" Ind. Eng. Chem. Res. **42**, 6518 (2003).
4. Sinor Synthetic Fuels Report Volume 6 No. 2 April 1999 page126. Available at http://edj.net/sinor/SFR4-99art7.html.
5. P.J.M. Tijm, F.J. Waller, D.M. Brown "Methanol Technology Developments for the New Millenium" Appl. Catal. A 221, 275 (2001).
6. M, Marchiona, M. DiGirolamo, L. Tagliabue, M.J. Spangler, T.H. Fleisch "A Review of Low Temperature Methanol Synthesis" Studies in Surface Science and Catalysis **119**, 539 (1998).
7. K.M. Vanden Bussche, G.F. Froment "A Steady-State Kinetic Model for Methanol Synthesis and the Water Gas Shift Reaction on a Commercial $Cu/ZnO/Al_2O_3$ Catalyst" J. Catal. **161**, 1 (1996).
8. D. Mignard, M. Sahibzada, J.M. Duthie, H.W. Whittington "Methanol Synthesis from Flue-Gas CO_2 and Renewable Electricity: A Feasibility Study" Int. J. Hydrogen Energy **28**, 455 (2003).
9. See for example M. Saito, T. Fujitani, M. Takeuchi, T. Watanabe "Development of Copper/Zinc Oxide-Based Multicomponent Catalysts for Methanol Synthesis from Carbon Dioxide and Hydrogen" Appl. Catal. A **138**, 311 (1996).
10. See for example C. Yang, Z. Ma, N. Zhao, W. Wei, T. Hu, Y. Sun "Methanol Synthesis from CO_2-Rich Syngas over a ZrO_2 doped CuZnO Catalyst" Catal. Today **115**, 222 (2006); J. Toyir, P.R. de la Piscina, J.L.G. Fierro, N. Homs "Catalytic Performance for CO_2 Conversion to Methanol of Gallium-Promoted Copper-Based

Catalysts : Influence of Metallic Precursors" Appl. Catal. B **34**, 255 (2001); and M. Lachowska, J. Skrzypek "Ga, Mn and Mg Promoted Coper/Zinc/Zirconia-Catalysts for Hydrogenation of Carbon Dioxide to Methanol" Studies in Surface Science and Catalysis **153**, 173 (2004).

11. T. Kubota, I. Hayakawa, H. Mabuse, K. Mori, K. Ushikoshi, T. Watanabe, M. Saito "Kinetic Study of Methanol Synthesis from Carbon Dioxide and Hydrogen" Appl. Organometal. Chem, **15**, 121 (2001).

12. J. Erena, R. Garoña, J.M. Arandes, A. Aguayo, J. Bilbao "Direct Synthesis of Dimethyl Ether from (H_2+CO) and (H_2+CO_2) Feeds. Effect of Feed Composition" Int. J. Chem. Reactor Eng. 3, Article A44 (2005).

13. A.T. Aguayo, J. Erena, I. Sierra, M. Olazar, J. Bilbao "Deactivation and Rgeneration of Hybrid Catalysts in the Single-Step Synthesis of Dimethyl Ether from Syngas and CO_2" Catal. Today **106**, 265 (2005).

14. See for example X.D. Peng, B.A. Toseland, P.J.A. Tijm "Kinetic Understanding of the Chemical Synergy under LPDME™ Conditions – Once-Through Applications" Chem Engr. Sci. **54**, 2787 (1999).

Appendix A. Reactor Modeling (Bussche and Froment)

The model of Bussche and Froment[**] is based on two reactions of CO_2 1) methanol synthesis, and 2) the water gas shift reaction.

1) $CO_2 + 3H_2 \leftrightarrow CH_3OH + H_2O$
2) $CO_2 + H_2 \leftrightarrow CO + H_2O$

The respective reaction rates are given by the two following equations which have been subjected to validation with experimental data.

$$\frac{d\beta_1}{dz} = r_1 = \frac{k_4 P_{CO_2} P_{H_2} \left[1 - \frac{1}{k_{E1}} \left(\frac{P_{H_2O} P_{CH_3OH}}{P_{H_2}^3 P_{CO_2}} \right) \right]}{\left[1 + k_3 \left(\frac{P_{H_2O}}{P_{H_2}} \right) + k_1 \sqrt{P_{H_2}} + k_2 P_{H_2O} \right]^3}$$

$$\frac{d\beta_2}{dz} = r_2 = \frac{k_5 P_{CO_2} \left[1 - \frac{1}{k_{E2}} \left(\frac{P_{H_2O} P_{CO}}{P_{H_2}^3 P_{CO_2}} \right) \right]}{\left[1 + k_3 \left(\frac{P_{H_2O}}{P_{H_2}} \right) + k_1 \sqrt{P_{H_2}} + k_2 P_{H_2O} \right]}$$

The reaction rate constants (k_1-k_5) and the equilibrium constants (k_{E1} and k_{E2}) are given as follows.

$k_1 = 0.499 e^{17197/RT}$ $\qquad\qquad$ $k_{E1} = 10^{(3066/T)-10.592}$

$k_2 = 6.62 \times 10^{-11} e^{124119/RT}$ $\qquad$ $k_{E2} = 10^{(-2073/T)+2.029}$

$k_3 = 3453.38$

$k_4 = 1.07 e^{36696/RT}$

$k_5 = 1.22 \times 10^{10} e^{-94765/RT}$

Following the method of Sinadinović-Fišer et al.[††], the number of moles of each reactant and product can be calculated from the materials balance as

$n_{CO_2} = n_{CO_2}^0 - \beta_1 - \beta_2$ $\qquad\qquad$ $n_{CO} = n_{CO}^0 + \beta_2$

[**] K.M. Vanden Bussche, G.F. Froment "A Steady-State Kinetic Model for Methanol Synthesis and the Water Gas Shift Reaction on a Commercial Cu/ZnO/Al$_2$O$_3$ Catalyst" J. Catal. **161**, 1 (1996).
[††] S.V. Sinadinović-Fišer, M.R. Janković, R.Ž, Radičević "Simulation of the Fixed-bed Reactor for Methanol Synthesis" Petrol. and Coal **43**, 31 (2001).

$$n_{H_2} = n_{H_2}^0 - 3\beta_1 - \beta_2 \qquad\qquad n_{H_2O} = n_{H_2O}^0 + \beta_1 + \beta_2$$

$$n_{CH_3OH} = n_{CH_3OH}^0 + \beta_1 \qquad\qquad n_{total} = n_{CO_2} + n_{H_2} + n_{CH_3OH} + n_{CO} + n_{H_2O} + n_{inert}$$

Where n_i^0 is the initial (feed) amount of component i. The partial pressures are then:

$$P_i = P\left(\frac{n_i}{n_{total}}\right)$$

The data for figures 9-14 were produced by manually integrating the rate equations and solving the material balances for discrete increments of Δz. Increments in Δz of 0.01 units were typically sufficiently small to converge to a consistent result.

Appendix B. Reactor Modeling (Kubota et al.)

The model of Kubota et al.[‡‡] is based on the same two reactions of CO_2 in the model of Bussche and Froment 1) methanol synthesis, and 2) the water gas shift reaction. The reaction equations were derived based on the assumption that methanol is produced through formate and methoxy intermediates and that the surface reaction between the formate and adsorbed hydrogen atoms is the rate determining step. The RWGS reaction was presumed to proceed through direct decomposition of CO_2 to CO on the copper surface. The resulting equations were simplified by assuming that the square root of the H_2 partial pressure is essentially constant, and that the partial pressure of H_2O is very small relative to the partial pressure of H_2 ($P_{H2O}/P_{H2} \approx 0$).

The respective reaction rates are given by the two following equations

$$\frac{d\beta_1}{dz} = R_M = \frac{k_M P_{CO_2} P_{H_2} \left[1 - \frac{1}{K_M} \left(\frac{P_{H_2O} P_{CH_3OH}}{P_{H_2}^3 P_{CO_2}} \right) \right]}{\left(1 + K_{CO_2} P_{CO_2} + K_{H_2O} P_{H_2O} \right)^2}$$

$$\frac{d\beta_2}{dz} = R_R = \frac{k_R P_{CO_2} \left[1 - \frac{1}{K_R} \left(\frac{P_{H_2O} P_{CO}}{P_{H_2} P_{CO_2}} \right) \right]}{1 + K_{CO_2} P_{CO_2} + K_{H_2O} P_{H_2O}}$$

The reaction rate constants (k_M, k_R), adsorption equilibrium constants (K_{CO2} and K_{H2O}) and equilibrium constants (K_M and K_R), are given as follows.

$$k_M = 3.261 \times 10^4 e^{-32093/RT}$$
$$k_R = 1.3831 \times 10^{12} e^{-113390/RT}$$
$$K_{CO_2} = 0.741$$
$$K_{H_2O} = 1.44511 \times 10^{-8} e^{82215.3/RT}$$

$$K_M = 10^{(7087/T)-19.499}$$
$$K_R = 10^{(-4778/T)+4.639}$$

Data for a $Cu/ZnO/ZrO_2/Al_2O_3/SiO_2$ catalyst was fitted to obtain the values for the rate constants and adsorption equilibrium constants.

The data for figures B1-B5 were produced by applying the method of Sinadinović-Fišer[§§] et al. and manually integrating the rate equations and solving the material balances for discrete increments of Δz. Increments in Δz of 0.00001 to 0.0001 units were typically sufficiently small to converge to a consistent result.

[‡‡] T. Kubota, I. Hayakawa, H. Mabuse, K. Mori, K. Ushikoshi, T. Watanabe, M. Saito "Kinetic Study of Methanol Synthesis from Carbon Dioxide and Hydrogen" Appl. Organometal. Chem, **15**, 121 (2001).
[§§] S.V. Sinadinović-Fišer, M.R. Janković, R.Ž, Radičević "Simulation of the Fixed-bed Reactor for Methanol Synthesis" Petrol. and Coal **43,** 31 (2001).

Unlike the Bussche/Froment model, the Kubota model does not indicate inhibition of the reaction by water when feeding CO_2 and H_2. It is not clear whether this is indicative of the catalyst having enhanced water tolerance, or whether this is simply the result of extending the model past its predictive capability. Certainly as can be seen in Figure B4 as conversion increases for CO_2 and H_2 feed, the assumption that $P_{H2O}/P_{H2} \approx 0$ would begin to break down. Thus experimental validation will be required.
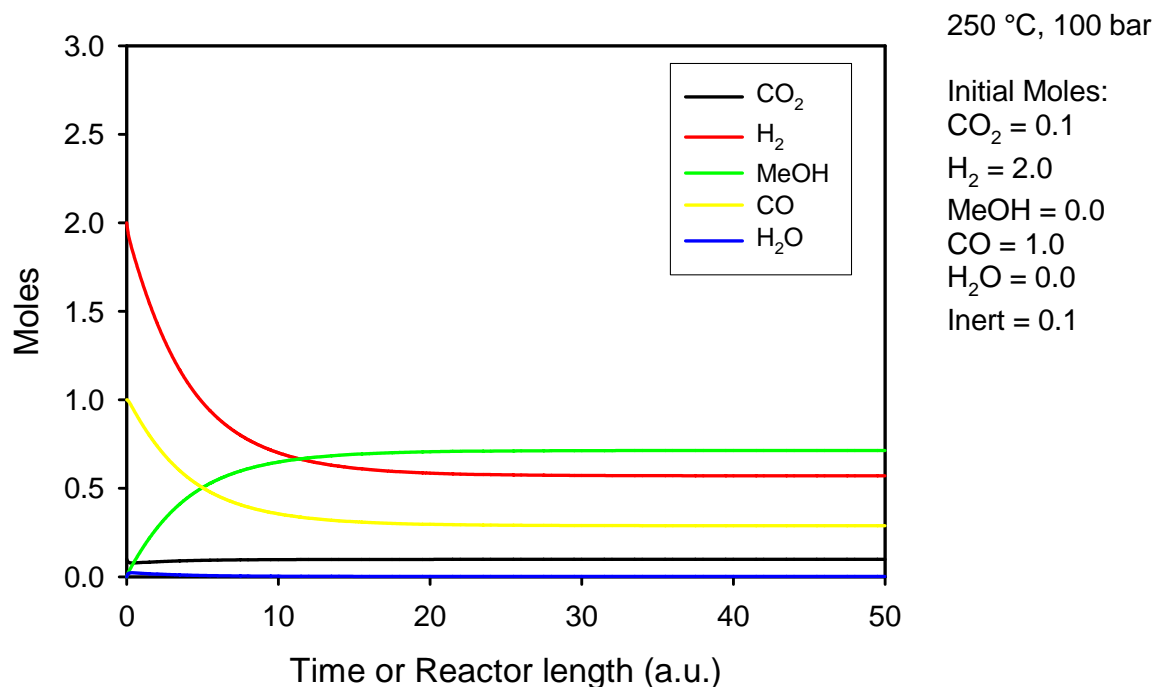

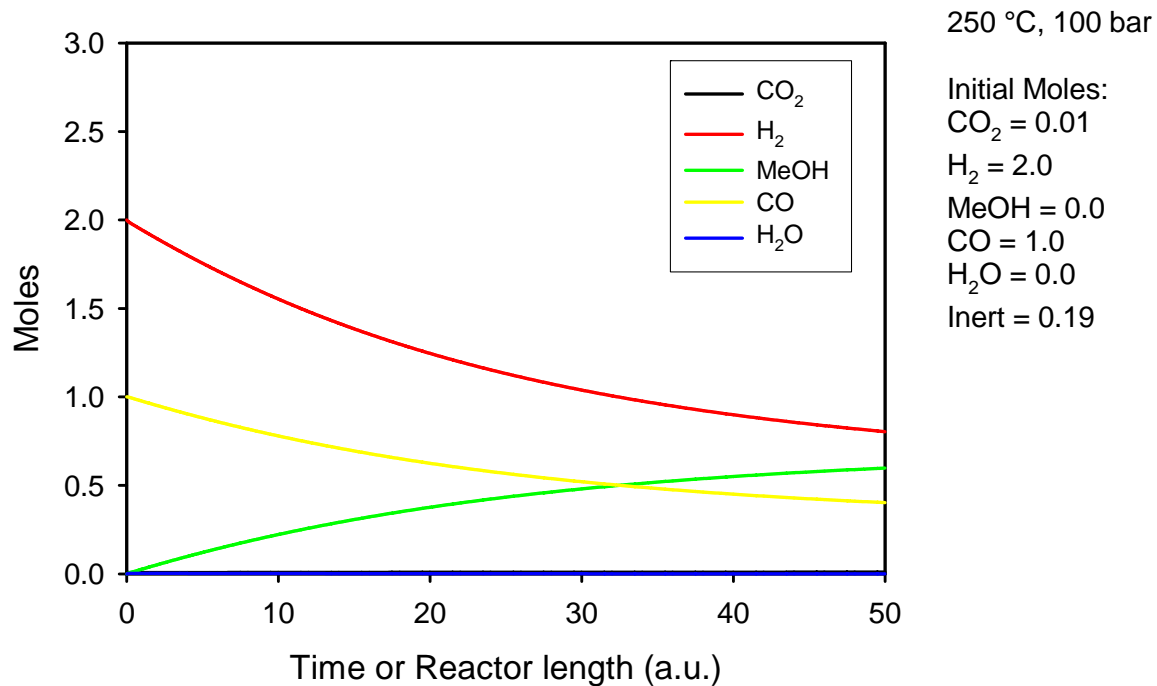**Figure B1.** Calculated conversion of CO_2-containing synthesis gas to methanol over $Cu/ZnO/Al_2O_3$ (Kubota Model).

250 °C, 100 bar

Initial Moles:
CO_2 = 0.01
H_2 = 2.0
MeOH = 0.0
CO = 1.0
H_2O = 0.0
Inert = 0.19

Figure B2. Calculated conversion of synthesis gas to methanol over $Cu/ZnO/Al_2O_3$. Syngas feed is dry and CO_2 deficient (Kubota Model).

250 °C, 100 bar

Initial Moles:
CO_2 = 0.01
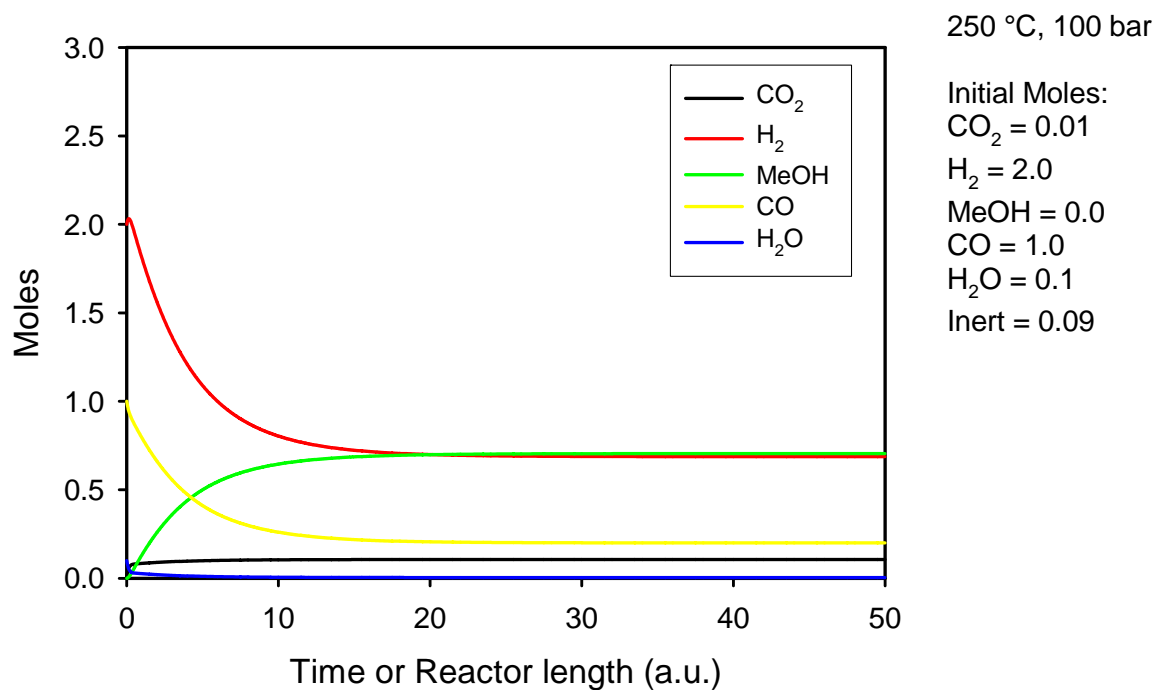H_2 = 2.0
MeOH = 0.0
CO = 1.0
H_2O = 0.1
Inert = 0.09

Figure B3. Calculated conversion of synthesis gas to methanol over $Cu/ZnO/Al_2O_3$. Syngas feed is CO_2 deficient, but moist (Kubota Model).
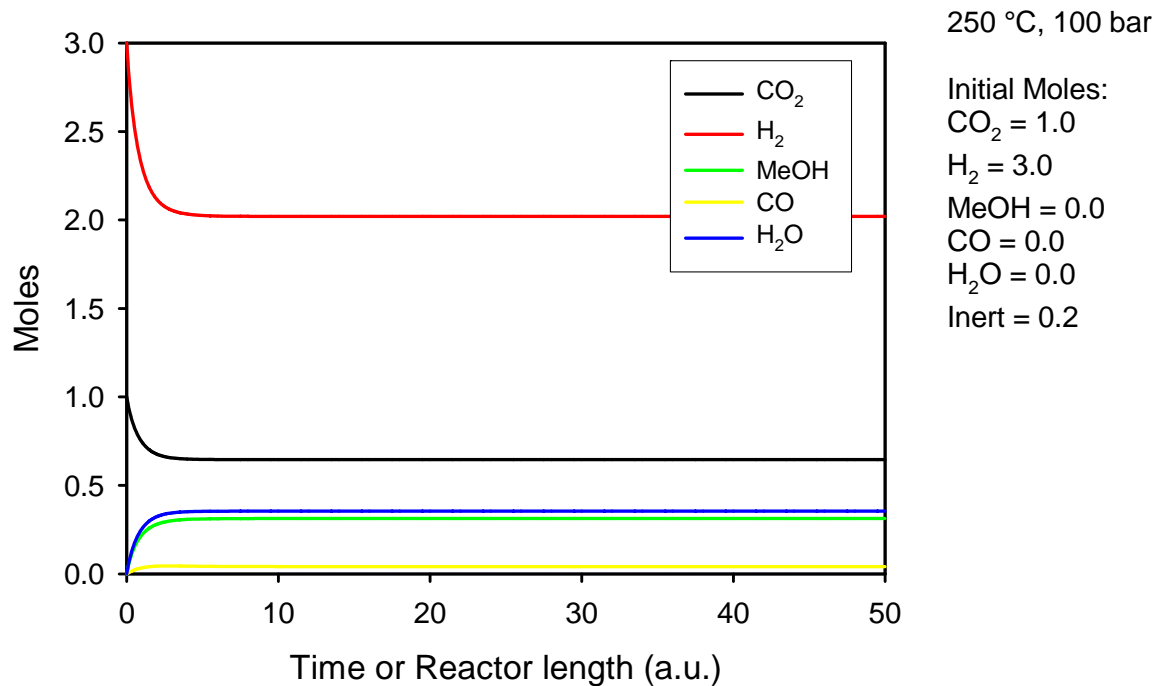
250 °C, 100 bar

Initial Moles:
CO_2 = 1.0
H_2 = 3.0
MeOH = 0.0
CO = 0.0
H_2O = 0.0
Inert = 0.2

Figure B4. Calculated conversion of dry 3:1 H_2:CO_2 mixture to methanol over Cu/ZnO/Al_2O_3 (Kubota Model).

250 °C, 100 bar

Initial Moles:
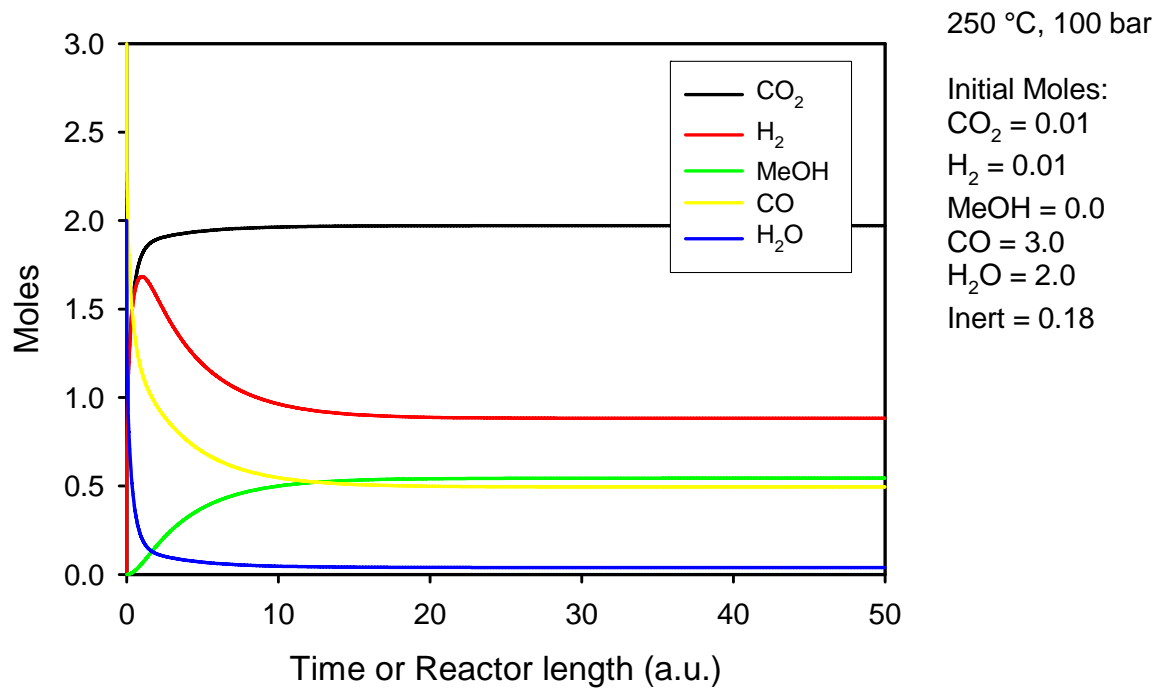CO_2 = 0.01
H_2 = 0.01
MeOH = 0.0
CO = 3.0
H_2O = 2.0
Inert = 0.18

Figure B5. Calculated conversion of 3:2 CO:H_2O mixture to methanol over Cu/ZnO/Al_2O_3 (Kubota Model).

DISTRIBUTION:

10	MS 1349	James Miller, 1815
1	MS 1349	Lindsey Evans, 1815
1	MS 1349	Eric Coker, 1815
1	MS 1349	Rick Kemp, 1815
1	MS 1349	Bill Hammetter, 1815
1	MS 0887	Justine Johannes 1810
1	MS 0887	Duane Dimos, 1800
1	MS 0734	Andrea Ambrosini, 6338
1	MS 0734	Ellen Stechel, 6338
1	MS 1127	Rich Diver, 6335
1	MS 1127	Nathan Siegel, 6337
1	MS 1110	Jeff Nelson, 6330
1	MS 0406	Fred Gelbard, 5713
1	MS 1415	Roland Stumpf, 1114
1	MS 0123	LDRD, Donna Chavez, 1011
1	MS 0899	Technical Library, 9536 (electronic copy)